RAA 2018 Vol. **18** No. **12**, 156(8pp) doi: 10.1088/1674–4527/18/12/156

http://www.raa-journal.org *http://iopscience.iop.org/raa*

Research in Astronomy and Astrophysics

Gaia calibrated UV luminous stars in LAMOST

Yu Bai[1], Ji-Feng Liu[1,2] and Song Wang[1]

[1] Key Laboratory of Optical Astronomy, National Astronomical Observatories, Chinese Academy of Sciences, Beijing 100101, China; *ybai@nao.cas.cn*

[2] College of Astronomy and Space Sciences, University of Chinese Academy of Sciences, Beijing 100049, China

Received 2018 June 4; accepted 2018 July 5

Abstract We take advantage of *Gaia* Data Release 2 to present 275 and 1774 ultraviolet luminous stars in the far ultraviolet (FUV) and near ultraviolet (NUV), respectively. These stars exceed their expected values by 5σ with respect to over one million ultraviolet stars in the $\log g$ vs. $T_{\rm eff}$ diagram. Galactic extinction is corrected with a 3D dust map. In order to limit the Lutz-Kelker bias to an insignificant level, we select stars with relative uncertainties in luminosity less than 40% and trigonometric parallaxes less than 20%. We cross-identified our sample with the catalogs of RR Lyr stars and possible white dwarf main-sequence binaries, and find they compose $\sim$62% and $\sim$16% of our sample in the FUV and NUV, respectively. This catalog provides a unique sample to study stellar activity, spectrally unresolved compact main-sequence binaries and variable stars.

Key words: stars: activity — stars: general — ultraviolet: stars

1 INTRODUCTION

Most stars in our Galaxy are cool, emitting much of their electromagnetic radiation in the visible or near-infrared parts of the spectrum. These cool stars are defined by effective temperatures that are the thermal temperatures estimated from stellar photospheres. Higher regions of the stellar atmosphere (chromosphere, transition region and corona) are often dominated by more violent non-thermal physical processes mainly powered by the magnetic field (Bai et al. 2018a). These processes could produce high energy emissions in the ultraviolet (UV) or X-ray parts of the spectrum, and are associated with stellar activity.

This stellar activity could release a total energy higher than 10^{34} erg, which leads to discrepancies between observations and theoretical stellar models. Such discrepancy is severe in the UV band which is particularly sensitive to hot plasma emission ($\sim 10^4 - 10^6$ K). Therefore, the UV domain is ideal for investigating stellar activity and its availability has been explored for Sun-like stars (Findeisen et al. 2011) and M dwarfs (Jones & West 2016). An observational reference frame in the UV is essential to characterize stellar activity and further to identify truly peculiar stars, which are still poorly understood due to the previously small sizes of samples.

UV luminous stars are outliers that do not fit the UV reference frame. They are probably flaring stars that erupt due to magnetic reconnection. Their stellar magnetic field is thought to be generated and maintained by a stellar dynamo (Wright et al. 2011), or interaction in a binary star (Simon et al. 1980) or in a star-planet system (Ip et al. 2004). They could also be stars with very hot atmospheres, e.g., accreting pre-main sequence stars (Eaton & Herbst 1995), hot subdwarfs (Wang et al. 2017) and variable stars (Sesar et al. 2010; Bai et al. 2018a). The excessive UV emission may have originated from spectrally unresolved companions that are active late-type stars (Yang et al. 2017).

On the other hand, the main-sequence stars around compact objects that cannot be resolved by LAMOST spectra could also emit excessive UV photons (Jao et al. 2014). Such UV emission could originate from the accretion disks around white dwarfs (Gänsicke et al. 1997, 2001), neutron stars or black holes. The ratios between X-ray and UV luminosity are about 0.1-100 for quiescent accretion disks around neutron stars and black holes (Hynes & Robinson 2012; Cackett et al. 2013; Froning et al. 2014). This UV emission can provide important information to study compact objects in binary systems. Therefore, these UV outliers provide us a unique sample that enables us to further investigate the stellar activity and evolution of stars and binaries.

Bai et al. (2018a) presented a UV catalog of over three million stars selected from Data Release 3 of the LAMOST survey (Cui et al. 2012), in which about two-thirds were detected by the *Galaxy Evolution Explorer* (*GALEX*; Morrissey et al. 2007). We take advantage of this catalog to study the UV reference frame with the help of *Gaia* Data Release 2 (DR2; Gaia Collaboration et al. 2016, 2018a). We present the data for calculation of UV luminosity in Section 2. The selection of UV luminous stars is presented in Section 3. Section 4 gives a summary.

2 DATA

We calculate average magnitudes in Bai et al. (2018a) and extract the stellar parameters of effective temperature ($T_{\rm eff}$) and surface gravity (log g). *Gaia* DR2 provides parallaxes that can be used to obtain distance information. The UV stars are cross-matched to *Gaia* DR2 with a match radius of $2''$. Estimating distance directly from the trigonometric parallax may suffer from the Lutz-Kelker bias (LKB), which was discussed in detail by Trumpler & Weaver (1953), and then parametrically formalized by Lutz & Kelker (1973). The effect is defined as an offset between the average absolute magnitudes for classes of stars as determined from trigonometric parallax samples and the true mean absolute magnitude for that stellar class (Lutz & Kelker 1973; Sandage et al. 2016). The bias is found to be significant for stars with relatively high parallax uncertainty, $\sigma_\pi/\pi \gtrsim 20\%$. However, systematic correction for this bias has been challenged in more recent years (Smith 2003; van Leeuwen 2007; Francis 2014). In order to limit the LKB to an insignificant level, we select stars with relatively small uncertainties in their trigonometric parallaxes. We could also constrain the classification bias of our sample with this selection criterion (see Bai et al. (2018b) for details).

The Bayesian method developed by Burnett & Binney (2010) and Binney et al. (2014) has been used for stars in the RAVE survey, which has demonstrated the ability to obtain accurate distance and extinction. Wang et al. (2016) measured extinctions and distances using this method for stars with valid stellar parameters in the second data release of the LAMOST survey. They used the spectroscopic parameters $T_{\rm eff}$, [Fe/H] and $\log g$, and 2MASS photometry to compute posterior probabilities with the Bayesian method. We compare their distances to those from *Gaia* in Figure 1. Here, we plot the stars with relative uncertainties less than 20% for the *Gaia* distances and do not constrain the relative uncertainties of Bayesian distances (Bai et al. 2018a). Distances from the Bayesian method are underestimated, probably due to uncertainties in the stellar parameters if they are not well constrained in the LAMOST pipeline (Wu et al. 2011). The trigonometric parallaxes in *Gaia* DR2, however, have good consistency with those from other methods (Gaia Collaboration et al. 2018b).

Galactic extinction plays a much larger role for far UV (FUV)/near UV (NUV) than for other bands (Cardelli et al. 1989). In order to correct this extinction, we use the three-dimensional (3D) dust map from Green et al. (2015), which gives $E(B-V)$ as a function of the distance and position. In conjunction with distances derived from *Gaia* parallaxes, we estimate the reddening in the line of sight for each star in our sample. We adopt the extinction coefficients from Yuan et al. (2013) and Jordi et al. (2010) for the FUV/NUV and *Gaia* bands, respectively. All the magnitudes presented hereafter are extinction-corrected. The Hertzsprung-Russell (HR) diagram for our sample (Fig. 2, left panel) contains 1 474 479 UV stars with valid distances and extinctions, in which the magnitudes and colors are extracted from *Gaia* DR2.

Using the trigonometric parallaxes from *Gaia* DR2, we calculate the luminosities in FUV/NUV. We select stars with relative uncertainty in $L_{\rm UV}$ less than 40% and find that their $\sigma_\pi/\pi < 20\%$. In this case, the LKB in our sample does not significantly influence the luminosity. There are 85 444 and 1 271 863 stars satisfying the criteria in FUV and NUV, respectively (Fig. 2, right panel). The number of stars with $\mathrm{M}_G < -2$ is less than that in the full sample; this may be due to the LKB in which the absolute magnitudes are overestimated. We present an HR-like diagram of these stars in Figure 3. The stars become luminous with increasing effective temperatures, which is similar to the results of Shkolnik (2013) and Bai et al. (2018a).

3 RESULT

3.1 UV Luminous Stars

This luminosity catalog provides a wealth of information for the study of stellar UV emission, and enables us to investigate the UV reference frame. We bin the stars in

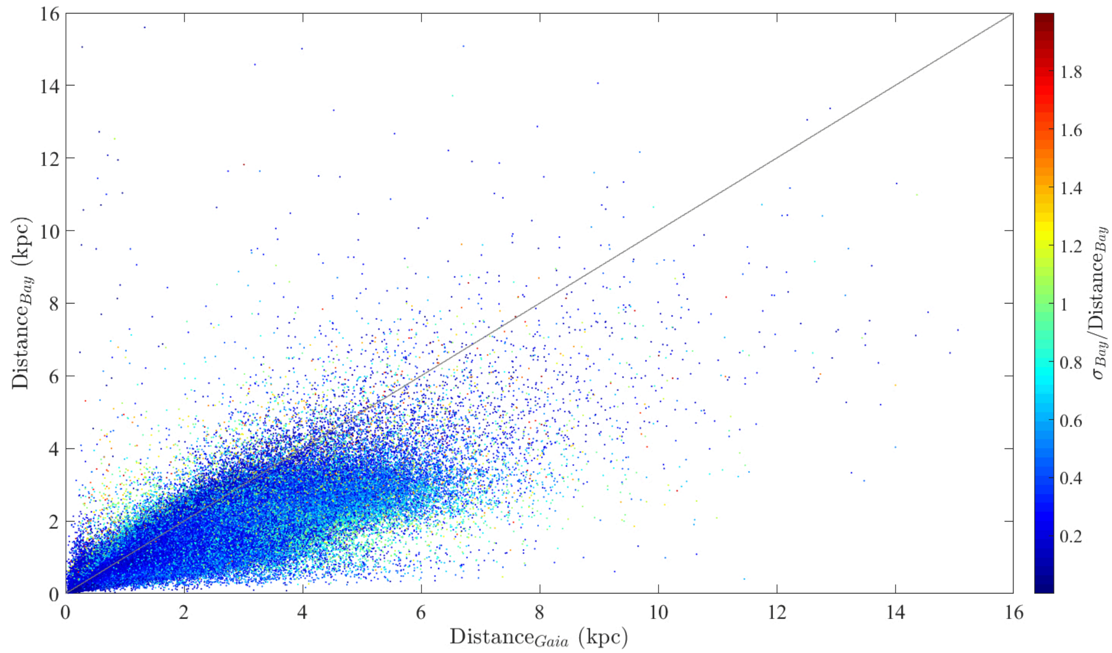

Fig. 1 Comparison of distances estimated with the Bayesian method with those from *Gaia*. The color bar stands for the relative uncertainties in the Bayesian distances.

the $\log g$ vs. $T_{\rm eff}$ diagram with steps of 0.5 in $\log g$ and 100 K in $T_{\rm eff}$. The distribution of luminosity in each bin is fitted with a Gaussian function if the number of stars in the bin is more than 200. We then select stars that fall outside the normal ranges (5σ) of the Gaussian function. Here σ stands for the standard deviation of the Gaussian fit. The fitting results are displayed in Figure 4, and listed in Tables 1 and 2. The selection yields 275 luminous and 17 quiet stars in FUV, and 1774 luminous and 943 quiet stars in NUV. The luminosity values for these stars are listed in Tables 3 and 4.

We plot the luminosity vs. $T_{\rm eff}$ in the left panels of Figure 5. The UV luminous and quiet stars are located along the main sequence, when $T_{\rm eff} \gtrsim 5500$ K. For the stars with $T_{\rm eff} \lesssim 5500$ K, since they are no longer dominated by dwarfs, the distributions for the UV luminous and quiet stars are not located along the main sequence. We find that the UV quiet stars are consistent with the theoretical model (the contours in Fig. 5). These stars do not show obvious UV excesses above the emission predicted by the model. The luminosity vs. F(N)UV $-H$ is displayed in the right panels of Figure 5. The UV luminous and quiet stars are not distributed along the main sequence, because the UV $-$ infrared (IR) colors of the early type stars depend on $T_{\rm eff}$ (Bai et al. 2018a). Again, colors of the UV quiet stars are consistent with theoretical colors from the model.

3.2 What Are These Stars?

RR Lyrae (RR Lyr) stars are pulsating periodic horizontal branch variables with great variation in the UV, spanning a range of 2–5 mag (Wheatley et al. 2012), making them more likely to be strong UV emitters. We cross-match the UV luminous stars with the RR Lyr catalogs in Sesar et al. (2010), Drake et al. (2013), Abbas et al. (2014) and the Simbad archive data with a match radius of $2''$. There are 46 and 69 RR Lyr stars that are luminous in FUV and NUV, respectively. The probabilities of matching an RR Lyr star are $\sim$17% and $\sim$4% in the FUV and NUV from our sample respectively, and higher than that in the UV star catalog, $\lesssim$0.1% (Bai et al. 2018a), indicating that the RR Lyr stars are likely to emit excessive UV photons.

The binaries composed of non-degenerate stars and white dwarfs are probably unresolved by LAMOST spectra, and these binaries may become more luminous in the UV than what is expected for the secondary stars. Bai et al. (2018a) presented a sample of potential white dwarf main-sequence binaries based on their density distributions in FUV $-$ NUV vs. $W1 - W2$, which are extracted from the *GALEX* and *WISE* catalogs. We cross-match the UV luminous stars with this sample, and find 123 and 213 stars in the FUV and NUV corresponding to $\sim$45% and $\sim$12% of our sample respectively. If these stars are white dwarf binaries, their UV luminosities are

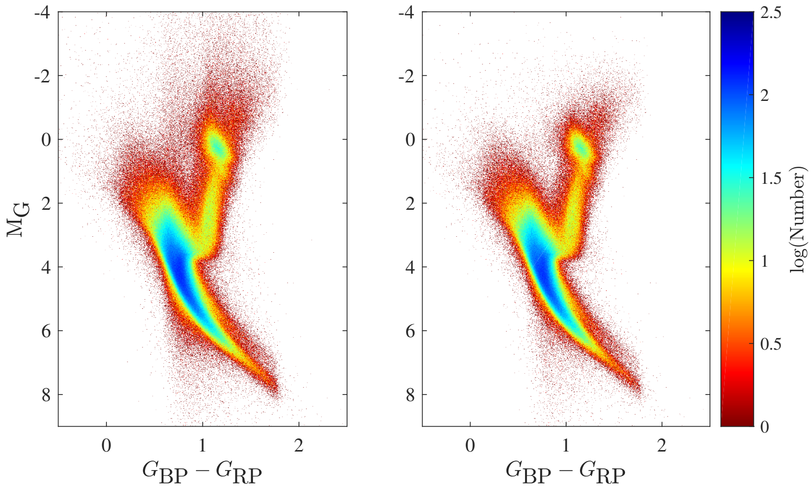

Fig. 2 M_G vs. $G_{BP} - G_{RP}$ distribution for the full UV star sample (*left panel*) and for the stars with relative uncertainty in L_{UV} less than 40% (*right panel*). The color bar stands for the density in log scale.

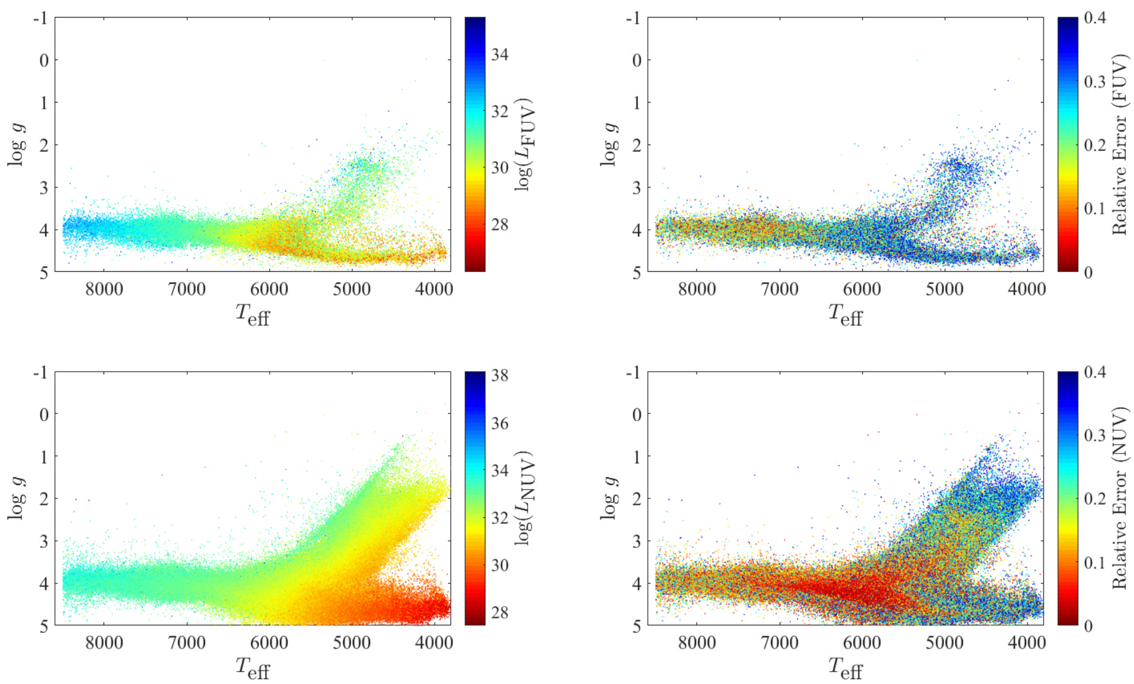

Fig. 3 HR-like diagrams. The color bars stand for luminosities in the FUV and NUV in the left two panels and the relative uncertainties of the luminosities in the right two panels.

dominated by the accretion disks or hot atmospheres of the white dwarfs.

The FUV − NUV vs. $W1-W2$ diagram is useful for selecting white dwarf plus M dwarf binaries, since their emissions are mainly in the UV and IR bands, respectively. For binaries with secondary stars earlier than M, the IR color is not sensitive enough to distinguish white dwarf binaries from single stars. We present the spectrum of a UV luminous star as an example in Figure 6. It is spectrally identified as an F star with $T_{eff} = 6298$ K and $\log g = 4.05$. Its FUV luminosity exceeds the expected value by 5.9σ. The three emission lines marked in blue correspond to the night sky emission lines from mercury. The emission line signified by red is Fe II λ6113 which originates from hot thin gas, and has also been detected in nova spectra, e.g., Cyg 2014 [1] and V445 Puppis (Iijima & Nakanishi 2008). This star is probably part of a binary system that includes a spectrally unresolved white dwarf which increases the FUV emission and the Fe II line.

[1] *http://www.astrosurf.com/aras/Aras_DataBase/DataBase.htm*

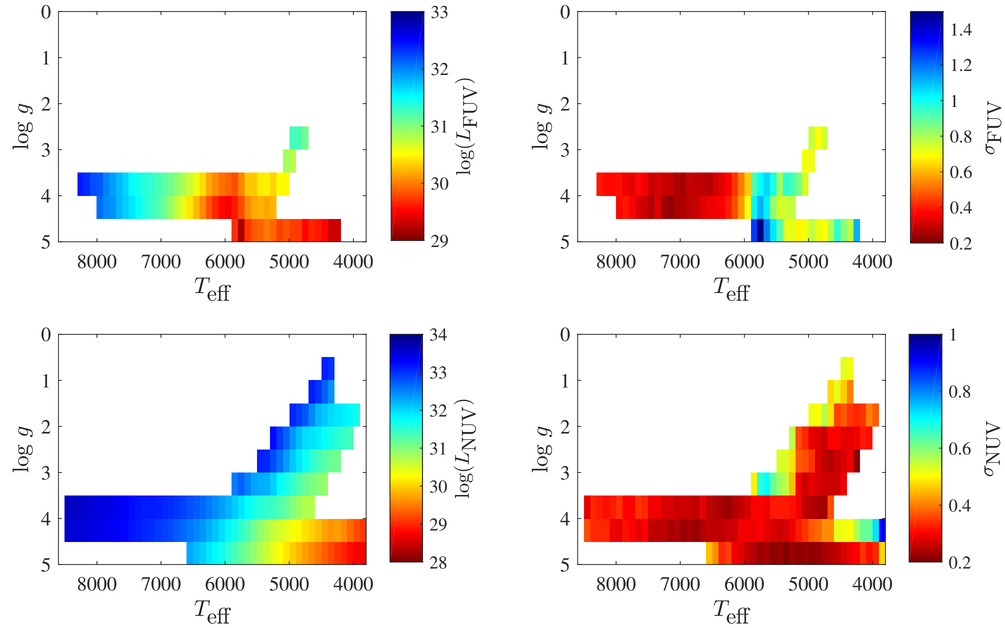

Fig. 4 Distributions of the fit results in the FUV (*top panels*) and NUV (*bottom panels*). The color bars stand for μ and σ from the Gaussian fits in the bins.

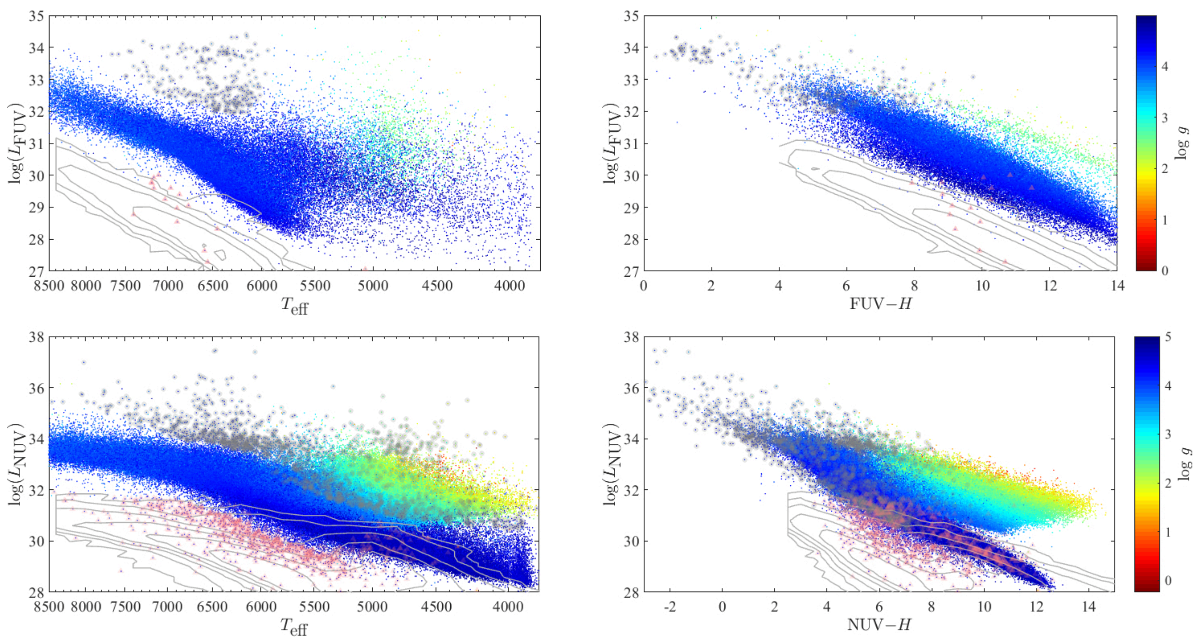

Fig. 5 UV luminosity vs. $T_{\rm eff}$ (*left panels*) and UV $-H$ color (*right panels*). The UV luminous stars are displayed as *grey points* and the UV quiet stars are represented as *pink triangles*. The contours stand for distributions from the BT-Cond grid (Allard & Freytag 2010) of the PHOENIX photospheric model (Hauschildt et al. 1999). The color bars correspond to values of log g.

This implies that there are some potential white dwarf $-$ G dwarf binaries and white dwarf $-$ F dwarf binaries in our sample, which require additional optical colors to identify them.

There may also be some active stars or active non-degenerate binaries in our sample. They are probably fast rotating stars with strong stellar activity (Reiners 2012), or they may have magnetic field lines that interconnect with their companion (Simon et al. 1980). They also could be very young stars or hot subdwarfs with excessive UV emission from their hot atmospheres. Neutron star and black hole binaries are not ruled out, but we need multi-band information from radio to X-ray to positively identify them.

Table 1 Fit Result in the FUV

Ind	$T_{\rm eff}$	log g	σ	μ	Num	High Num	Low Num
(1)	(2)	(3)	(4)	(5)	(6)	(7)	(8)
1	4250	4.75	1.11±0.11	29.30±0.10	205	0	0
2	4350	4.75	0.77±0.06	29.29±0.06	243	0	0
3	4450	4.75	0.84±0.09	29.51±0.08	245	0	0
4	4550	4.75	0.95±0.06	29.59±0.06	243	0	0
5	4650	4.75	0.78±0.06	29.64±0.06	312	0	0
6	4750	2.75	0.75±0.07	31.07±0.07	260	0	0
7	4750	4.75	0.69±0.08	29.52±0.08	337	0	0
8	4850	2.75	0.69±0.06	31.23±0.06	253	0	0
9	4850	4.75	0.71±0.03	29.73±0.03	372	0	0
10	4950	2.75	0.76±0.04	31.23±0.04	200	0	0
11	4950	3.25	0.71±0.08	30.79±0.08	216	0	0
12	4950	4.75	0.77±0.04	29.74±0.04	440	0	0
13	5050	3.25	0.70±0.03	30.86±0.03	226	0	1
14	5050	3.75	0.74±0.04	30.48±0.04	212	0	0

Notes: (1) The index of the bin. (2) The median $T_{\rm eff}$ in the unit of K. (3) The median $\log g$. (4) The standard deviation of the Gaussian fit in erg s^{-1}. (5) The center of the distribution from the Gaussian fit in erg s^{-1}. (6) The number of stars in the bin. (7) The number of stars with a lower limit of luminosity 5σ higher than the center of the Gaussian fit. (8) The number of stars with a higher limit of luminosity 5σ lower than the center of the Gaussian fit. This table is available in its entirety in electric form at *http://www.raa-journal.org/docs/Supp/ms4228Table1s.dat*.

Table 2 Fit Result in the NUV

Ind	$T_{\rm eff}$	log g	σ	μ	Num	High Num	Low Num
(1)	(2)	(3)	(4)	(5)	(6)	(7)	(8)
1	3850	4.25	0.90±0.10	29.07±0.09	247	0	0
2	3850	4.75	0.47±0.08	28.69±0.07	767	2	0
3	3950	1.75	0.37±0.03	31.63±0.03	397	0	0
4	3950	4.25	0.72±0.04	29.20±0.03	782	0	0
5	3950	4.75	0.33±0.03	28.73±0.03	1647	26	0
6	4050	1.75	0.40±0.03	31.78±0.03	570	2	0
7	4050	2.25	0.31±0.02	31.35±0.02	361	0	0
8	4050	4.25	0.62±0.05	29.37±0.05	529	0	0
9	4050	4.75	0.31±0.03	28.82±0.03	1939	28	0
10	4150	1.75	0.34±0.02	31.83±0.02	677	1	0
11	4150	2.25	0.32±0.02	31.42±0.02	796	3	0
12	4150	4.25	0.62±0.05	29.56±0.05	394	0	0
13	4150	4.75	0.34±0.02	28.95±0.02	2640	18	0
14	4250	1.75	0.33±0.02	31.89±0.02	778	3	1

Notes: The same as Table 1 but in NUV. This table is available in its entirety in electric form at *http://www.raa-journal.org/docs/Supp/ms4228Table2s.dat*.

4 SUMMARY

We present a catalog of 275 and 1774 luminous stars in the FUV and NUV, which exceed their expected values by at least 5σ. The reference frame is constructed with over one million LAMOST UV stars in the $\log g$ vs. $T_{\rm eff}$ diagram. We correct the extinction associated with UV emission using a 3D dust map with the distances from *Gaia* DR2. These UV luminous stars are selected with relative uncertainty in luminosity of less than 40% and that in trigonometric parallax of less than 20%, therefore they do not suffer significant LKB. We cross-match our sample with the catalogs of RR Lyr stars and possible white dwarf main-sequence binaries, and they constitute $\sim$62% and $\sim$16% of our sample in FUV and NUV, respectively.

This catalog provides an ideal sample to study stellar activity, compact main-sequence binaries and variable stars. These objects probably have optical spectra similar to normal stars, but have abnormal emission in UV. We

Table 3 The FUV Luminous and Quiet Stars

Ind (1)	Obsid (2)	$\log(L_{\rm FUV})$ (3)	$\log({\rm e}L_{\rm FUV})$ (4)	Flag (5)	Type (6)	Catalog (7)	WDMS (8)
13	55109124	27.07	26.65	0	Star		
41	128907057	32.86	32.20	1	Star		
42	133409048	33.28	32.48	1	RR Lyr	D	
42	231312031	32.76	32.26	1	RR Lyr	D	
43	260814117	34.40	33.48	1	Hot subdwarf		
44	31410196	32.65	32.13	1	RR Lyr	D	
44	75313026	32.53	32.07	1	RR Lyr		
44	145411088	32.50	31.92	1	RR Lyr	D	
44	148715114	32.65	32.12	1		D	
44	154611186	32.72	32.17	1	RR Lyr		
44	189215005	33.45	32.96	1	RR Lyr	D	
44	218501180	32.36	30.85	1	Star		1

Notes: (1) The index of the bin in which the stars are located. (2) The LAMOST obsid. (3) The luminosity in erg s^{-1}. (4) The uncertainty of the luminosity in erg s^{-1}. (5) The stars with the lower limit of luminosity higher than the center of the Gaussian fit by 5σ, Flag = 1, and the stars with the higher limit of luminosity lower than the center by 5σ, Flag = 0. (6) The types from the Simbad archive data. (7) The catalog flag. 'D'– Drake et al. (2013), 'S'– Sesar et al. (2010) and 'A'– Abbas et al. (2014). (8) The flag of the White Dwarf–Main Sequence candidates. This table is available in its entirety in electric form at *http://www.raa-journal.org/docs/Supp/ms4228Table3s.dat*.

Table 4 The NUV Luminous and Quiet Stars

Ind (1)	Obsid (2)	$\log(L_{\rm NUV})$ (3)	$\log({\rm e}L_{\rm NUV})$ (4)	Flag (5)	Type (6)	Catalog (7)	WDMS (8)
9	241109013	30.96	29.17	1	Binary		1
9	335113059	30.74	29.99	1	Star		1
19	318815093	27.92	27.34	0	High proper-motion Star		
30	267316208	33.62	33.01	1	Eclipsing binary of Algol type		
30	286203005	32.80	32.13	1			
30	269109099	29.77	29.21	0			
32	321511220	32.50	31.64	1	White Dwarf		1
40	210907122	30.86	29.42	1	X-ray source		1
111	217614072	34.19	33.76	1	RR Lyr	D	
121	151015067	33.65	32.89	1	RR Lyr	DA	

Notes: The same as Table 3 but in NUV. This table is available in its entirety in electric form at *http://www.raa-journal.org/docs/Supp/ms4228Table4s.dat*.

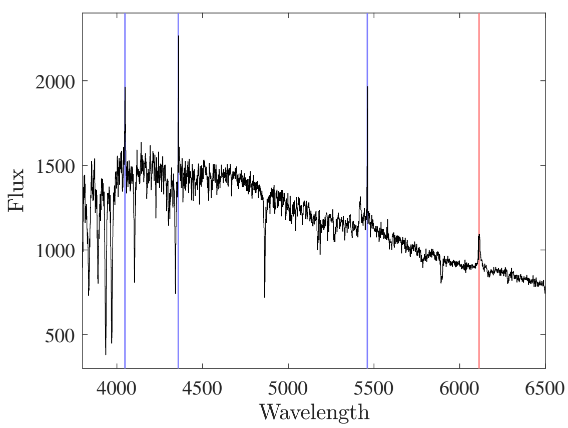

Fig. 6 LAMOST spectrum of a UV luminous star (Obsid = 167801105). The *red line* marks the Hg I emission lines, and the *blue lines* indicate the Fe II emission lines (*color online*).

will use the most recent data release from LAMOST to enlarge the sample and study them in detail to further shed light on the nature of these UV luminous stars.

Acknowledgements This work was supported by the National Program on Key Research and Development Project (Grant No. 2016YFA0400804) and the National Natural Science Foundation of China (NSFC) (Grant Nos. 11603038, 11333004, 11425313 and 11403056). Some of the data presented in this paper were obtained from the Mikulski Archive for Space Telescopes (MAST). STScI is operated by the Association of Universities for Research in Astronomy, Inc., under NASA contract NAS5-26555. Support for MAST for non-HST data is provided by the NASA Office of Space Science via grant NNX09AF08G and by other grants and contracts.

The Guo Shou Jing Telescope (the Large Sky Area Multi-Object Fiber Spectroscopic Telescope, LAMOST) is a National Major Scientific Project which was built by the Chinese Academy of Sciences, funded by the National Development and Reform Commission, and operated and managed by the National Astronomical Observatories, Chinese Academy of Sciences.

This work has made use of data from the European Space Agency (ESA) mission *Gaia* (*https://www.cosmos.esa.int/gaia*), which were processed by the *Gaia* Data Processing and Analysis Consortium (DPAC, *https://www.cosmos.esa.int/web/gaia/dpac/consortium*). Funding for the DPAC has been provided by national institutions, in particular institutions participating in the *Gaia* Multilateral Agreement.

References

Abbas, M. A., Grebel, E. K., Martin, N. F., et al. 2014, MNRAS, 441, 1230
Allard, F., & Freytag, B. 2010, Highlights of Astronomy, 15, 756
Bai, Y., Liu, J., Wicker, J., et al. 2018a, ApJS, 235, 16
Bai, Y., Liu, J., & Wang, S. 2018b, RAA (Research in Astronomy and Astrophysics), 18, 118
Binney, J., Burnett, B., Kordopatis, G., et al. 2014, MNRAS, 437, 351
Burnett, B., & Binney, J. 2010, MNRAS, 407, 339
Cackett, E. M., Brown, E. F., Degenaar, N., et al. 2013, MNRAS, 433, 1362
Cardelli, J. A., Clayton, G. C., & Mathis, J. S. 1989, ApJ, 345, 245
Cui, X.-Q., Zhao, Y.-H., Chu, Y.-Q., et al. 2012, RAA (Research in Astronomy and Astrophysics), 12, 1197
Drake, A. J., Catelan, M., Djorgovski, S. G., et al. 2013, ApJ, 765, 154
Eaton, N. L., & Herbst, W. 1995, AJ, 110, 2369
Findeisen, K., Hillenbrand, L., & Soderblom, D. 2011, AJ, 142, 23
Francis, C. 2014, MNRAS, 444, L6
Froning, C. S., Maccarone, T. J., France, K., et al. 2014, ApJ, 780, 48
Gaia Collaboration, Brown, A. G. A., Vallenari, A., et al. 2018a, arXiv:1804.09365
Gaia Collaboration, Prusti, T., de Bruijne, J. H. J., et al. 2016, A&A, 595, A1
Gaia Collaboration, Babusiaux, C., van Leeuwen, F., et al. 2018b, arXiv:1804.09378
Gänsicke, B. T., Beuermann, K., & Thomas, H.-C. 1997, MNRAS, 289, 388
Gänsicke, B. T., Szkody, P., Sion, E. M., et al. 2001, A&A, 374, 656
Green, G. M., Schlafly, E. F., Finkbeiner, D. P., et al. 2015, ApJ, 810, 25
Hauschildt, P. H., Allard, F., & Baron, E. 1999, ApJ, 512, 377
Hynes, R. I., & Robinson, E. L. 2012, ApJ, 749, 3
Iijima, T., & Nakanishi, H. 2008, A&A, 482, 865
Ip, W.-H., Kopp, A., & Hu, J.-H. 2004, ApJ, 602, L53
Jao, W.-C., Henry, T. J., Subasavage, J. P., et al. 2014, AJ, 147, 21
Jones, D. O., & West, A. A. 2016, ApJ, 817, 1
Jordi, C., Gebran, M., Carrasco, J. M., et al. 2010, A&A, 523, A48
Lutz, T. E., & Kelker, D. H. 1973, PASP, 85, 573
Morrissey, P., Conrow, T., Barlow, T. A., et al. 2007, ApJS, 173, 682
Reiners, A. 2012, Living Reviews in Solar Physics, 9, 1
Sandage, A., Beaton, R. L., & Majewski, S. R. 2016, PASP, 128, 064202
Sesar, B., Ivezić, Ž., Grammer, S. H., et al. 2010, ApJ, 708, 717
Shkolnik, E. L. 2013, ApJ, 766, 9
Simon, T., Linsky, J. L., & Schiffer, III, F. H. 1980, ApJ, 239, 911
Smith, H. 2003, MNRAS, 338, 891
Trumpler, R. J., & Weaver, H. F. 1953, Statistical astronomy (New York: Dover Publications)
van Leeuwen, F., ed. 2007, Astrophysics and Space Science Library, 350, Hipparcos, the New Reduction of the Raw Data
Wang, J., Shi, J., Pan, K., et al. 2016, MNRAS, 460, 3179
Wang, L., Gies, D. R., & Peters, G. J. 2017, ApJ, 843, 60
Wheatley, J., Welsh, B. Y., & Browne, S. E. 2012, PASP, 124, 552
Wright, N. J., Drake, J. J., Mamajek, E. E., & Henry, G. W. 2011, ApJ, 743, 48
Wu, Y., Luo, A.-L., Li, H.-N., et al. 2011, RAA (Research in Astronomy and Astrophysics), 11, 924
Yang, H., Liu, J., Gao, Q., et al. 2017, ApJ, 849, 36
Yuan, H. B., Liu, X. W., & Xiang, M. S. 2013, MNRAS, 430, 2188